HMG Advance Access published March 29, 2013

Human Molecular Genetics, 2013 **1–10**
doi:10.1093/hmg/ddt126

Phosphatidylserine increases *IKBKAP* levels in a humanized knock-in *IKBKAP* mouse model

Ron Bochner[1], Yael Ziv[1], David Zeevi[3], Maya Donyo[1], Lital Abraham[2], Ruth Ashery-Padan[1] and Gil Ast[1,*]

[1]Department of Human Molecular Genetics and Biochemistry, [2]Animal Facility, Sackler Faculty of Medicine, Tel Aviv University, Tel Aviv 69978, Israel and [3]Department of Computer Science and Applied Mathematics, Faculty of Mathematics and Computer Science, Weizmann Institute of Science, Rehovot, Israel

Received February 12, 2013; Revised and Accepted March 13, 2013

Familial dysautonomia (FD) is a severe neurodegenerative genetic disorder restricted to the Ashkenazi Jewish population. The most common mutation in FD patients is a T-to-C transition at position 6 of intron 20 of the *IKBKAP* gene. This mutation causes aberrant skipping of exon 20 in a tissue-specific manner, leading to reduction of the IκB kinase complex-associated protein (IKAP) protein in the nervous system. We established a homozygous humanized mouse strain carrying human exon 20 and its two flanking introns; the 3′ intron has the transition observed in the *IKBKAP* gene of FD patients. Although our FD humanized mouse does not display FD symptoms, the unique, tissue-specific splicing pattern of the *IKBKAP* in these mice allowed us to evaluate the effect of therapies on gene expression and exon 20 splicing. The FD mice were supplemented with phosphatidylserine (PS), a safe food supplement that increases mRNA and protein levels of *IKBKAP* in cell lines generated from FD patients. Here we demonstrated that PS treatment increases *IKBAKP* mRNA and IKAP protein levels in various tissues of FD mice without affecting exon 20 inclusion levels. We also observed that genes associated with transcription regulation and developmental processes were up-regulated in the cerebrum of PS-treated mice. Thus, PS holds promise for the treatment of FD.

INTRODUCTION

Familial dysautonomia (FD) is an autosomal recessive congenital neuropathy that occurs almost exclusively in the Ashkenazi Jewish population. The carrier frequency is remarkably high and ranges from 1 in 32 to as high as 1 in 18 in those of Polish descent (1). FD patients have abnormal development and survival of the sensory and autonomic nervous system with progressive depletion of unmyelinated sensory and autonomic neurons. The FD clinical spectrum includes gastrointestinal and cardiovascular dysfunction, vomiting crises, abnormal sensitivity to pain and temperature, lack of overflow tears, profuse sweating, recurrent pneumonia, hypertension and chronic renal disease (2–6). FD patients also suffer from progressive gait ataxia (7), which occurs as a result of the loss of proprioceptive inputs and progressive optic atrophy (8). Despite recent advances in patient management, ∼50% of patients die before the age of 40 years. The gene associated with the disease was linked to chromosome 9q31 and then identified as the *IKBKAP* gene. This gene encodes the IκB kinase complex-associated protein (IKAP). The point mutation observed in almost all FD patients (>99.5%) is a T-to-C transition at position 6 of the 5′ splice site (5′ss) of intron 20 (9,10). The mutation results in a shift from constitutive inclusion to alternative splicing of exon 20.

The shift to alternative splicing is due to reduction in U1 snRNA binding affinity to the 5′ss (11). The splicing defect in FD is tissue specific. Tissues from the brain and the nervous system express primarily mutant *IKBKAP* mRNA (skipping of exon 20), whereas other tissues express both wild-type (wt) and mutant mRNA in ratios that depend on the tissue type (2,12,13). The skipped isoform inserts a premature stop codon, leading to a considerable reduction in IKAP expression (no truncated protein is detected) in the nervous system (12,13).

The *IKBKAP* gene contains 37 exons and encodes a 150 kDa protein that is highly conserved in eukaryotes (14,15). Despite intensive research, the function of IKAP is still obscure. Based on

*To whom correspondence should be addressed. Tel: +972 36406893; Fax: +972 36409900; Email: gilast@post.tau.ac.il

homology to a yeast protein, ELP1, and co-purification with human Elongator (14), IKAP is thought to be a subunit of the Elongator complex, important for elongation by RNA polymerase II in the nucleus (14,16,17). However, IKAP is primarily a cytoplasmic protein, whereas transcription occurs in the nucleus. There is evidence that, in the cytosol, IKAP is involved in the regulation of the c-Jun N-terminal kinase signalling pathway (15), tRNA modification (18), exocytosis (19), cell adhesion, migration of cells and reorganization of actin in the cytoskeleton (20,21). We showed that IKAP also plays a role in oligodendrocyte differentiation and/or myelin formation (22) and in p53 activation (23). IKAP is also essential for vascular and neural development during embryogenesis (24).

Like its human counterpart, mouse *IKBKAP* encodes a protein of 1332 amino acids with a molecular weight of ~150 kDa. The mouse *IKBKAP* gene product contains 37 exons, and the protein has 80% amino acid identity with human IKAP. The mouse *IKBKAP* gene maps to chromosome 4 in a region that is syntenic to human chromosome 9q31.3 (12).

Several attempts to create an FD mouse model have been reported. The first, generated by Slaugenhaupt and co-workers (25), introduced a bacterial artificial chromosome (BAC) containing the human *IKBKAP* locus with the IVS20+T>C mutation into the mouse genome. In this mouse, the human gene was spliced in a tissue-specific manner that replicates the pattern seen in FD patient tissues. However, these mice are phenotypically normal and do not display any FD symptoms. A year later, Slaugenhaupt and co-workers (24) employed a knock-out strategy in an attempt to create a mouse with FD characteristics. Knock-out of *IKBKAP* resulted in embryonic lethality. No homozygous *IKBKAP* knock-out embryos ($IKBKAP^{-/-}$) survive beyond 12.5 days post-coitum. Morphological analyses of the $IKBKAP^{-/-}$ conceptus at different stages revealed abnormalities in both the visceral yolk sac and the embryo, including stunted extra-embryonic blood vessel formation, delayed entry into mid-gastrulation, disoriented dorsal primitive neural alignment and failure to establish the embryonic vascular system. Mice homozygous for the deletion of *IKBKAP* exon 20, established by Dragatsis and co-workers (26), are identical to null embryos and display growth retardation, severe cardiovascular defects and die early in embryogenesis, and hence do not constitute a mouse model for the disease. A year later, Dragatsis and co-workers (27) targeted the mouse *IKBKAP* gene through homologous recombination. Two distinct alleles were generated resulting in either loss of *IKBKAP* expression or expression of an mRNA lacking only exon 20. Homozygosity for either mutation caused developmental delays, cardiovascular and brain malformations and early embryonic lethality.

Here we generated a knock-in humanized mouse model in which human exon 20 and the two flanking introns, with IVS20+6T>C, replaced the reciprocal mouse genomic sequences. These mice are fully viable and do not show any of the FD symptoms. As exon 20 was skipped in certain mouse tissues, these mice can serve as a platform to examine whether a certain therapy affects mRNA splicing of exon 20 or the level of *IKBKAP* mRNA. We therefore used this mouse model to assess the impact on mRNA and protein levels of *IKBKAP* gene following a prolonged period of supplementation with a form of phosphatidylserine (PS), a major component of every living cell, especially neuronal cells (28). PS is used worldwide and is considered by the US Food and Drug Administration as a safe and lawful dietary supplement (29). PS significantly increased *IKBKAP* mRNA and IKAP protein levels in cells derived from FD patients (30).We used the supplement Sharp·PS® GOLD4508P, a proprietary conjugate of PS and docosahexaenoic acid (DHA), an omega-3 fatty acid. Sharp·PS® GOLD4508P resembles the functional form of natural brain PS and elevates DHA accessibility in the brain. This specific formula of PS increases the level of *IKBKAP* mRNA with only 5% of the effective concentration of PS (30).

Treatment of knock-in mice with the PS formulation caused elevation in both *IKBKAP* mRNA and IKAP protein levels in the examined tissues. These results demonstrate for the first time that oral treatment with PS elevates *IKBKAP* mRNA and IKAP protein levels in an *in vivo* system. We further examined the overall effect of PS on gene expression using microarray analysis of cerebrum and heart tissues. Our data show that PS administration resulted in the up-regulation of genes involved in transcription regulation and down-regulation of genes associated with mitochondrial function, specifically the respiratory chain, and with ribosome- and translation-associated genes. Our results show that PS can elevate *IKBKAP* mRNA and IKAP protein levels *in vivo* and indicate that PS warrants evaluation in FD patients.

RESULTS

Generation of a humanized knock-in *IKBKAP* mouse

In FD patients, exon 20 of the *IKBKAP* gene is predominantly skipped in the autonomous nervous system due to aberrant recognition of the 5′ splice site (9,13,31). The first step in our quest to generate a mouse model system was to generate human and mouse minigenes carrying the relevant genomic sequences and to examine the mode of splicing of these constructs in human and mouse cell lines. We also created two human–mouse chimeric minigenes in which mouse exon 20 and its two flanking introns were replaced by the corresponding human sequence. This substitution was carried out in both the wt and the IVS20+T>C contexts. We observed the same mode of splicing before and after the insertion of the IVS20+6T>C in mouse cells as seen in human cells (Supplementary Material, Fig. S1). We therefore generated mice in which exon 20 and its two flanking introns were replaced by the corresponding human sequence, containing the IVS20+6T>C (Fig. 1A). For simplicity, these $IKBKAP^{FDloxP/FDloxP}$ mice will be termed FD mice. The $IKBKAP^{FDloxP/+}$ mice were backcrossed to C57Bl/6J for five generations in order to obtain mice with a homogenous genetic background.

FD mice display tissue-specific alternative splicing

FD patients display a distinctive splicing pattern of *IKBKAP*. In brain and other neuronal tissues, exon 20 of *IKBKAP* is predominantly skipped, whereas in the rest of the tissues, it is alternatively spliced. This tissue-specific alternative splicing was shown not only in human but also in a mouse model containing a BAC of the human *IKBKAP* gene with the

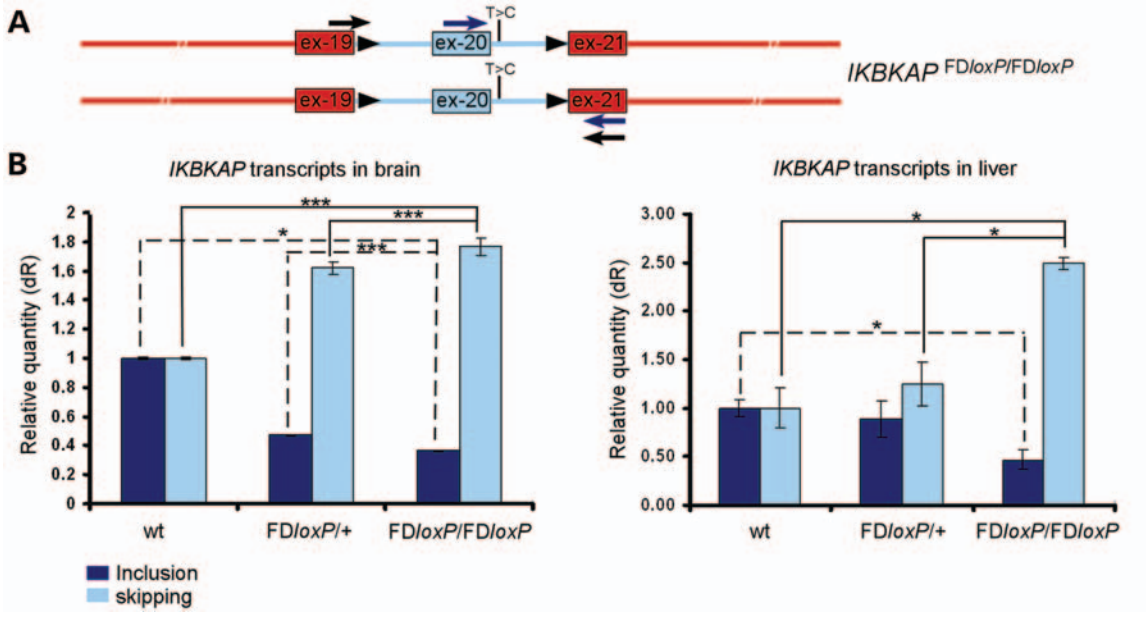

Figure 1. Tissue-specific alternative splicing pattern of exon 20 in *IKBKAP*$^{FDloxP/+}$ mice. (**A**) Schematic representation of the genotype of the humanized knock-in mouse. The FD IVS20+6T>C mutation is marked downstream to exon 20. Boxes and lines indicate exons and introns, respectively. Red represents mouse sequences, and celeste indicates human sequences. Short black arrowheads signify the two *loxP* sequences of 34 nt. Long black and blue arrowheads indicate the approximate location of primers that detect skipping and inclusion isoforms, respectively. The drawing is not to scale. (**B**) QPCR analysis of the two isoforms of the *IKBKAP* transcript. Inclusion isoform (wt) is in blue and skipping isoform (mutant) is in celeste. Data were normalized to inclusion or skipping levels of *IKBKAP* in wt mice and to *PPIA* housekeeping gene that showed the same level of expression among all three genotypes. Error bars represent SEM ($n = 3$). Statistically significant differences of inclusion and skipping isoforms among the three genotypes are indicated by dashed and solid lines, respectively. $^{*}P < 0.05$; $^{***}P < 0.005$; Student's *t*-test.

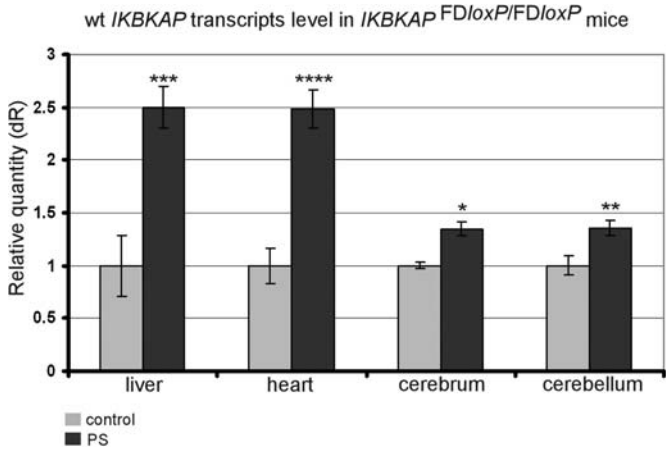

Figure 2. PS elevates wt *IKBKAP* mRNA levels in various tissues of *IKBKAP*$^{FDloxP/FDloxP}$ mice. QPCR analysis of the level of exon 20 inclusion isoform (wt) *IKBKAP* transcripts in the liver, heart, cerebrum and cerebellum of *IKBKAP*$^{FDloxP/FDloxP}$ mice supplemented with PS in comparison with mice given solvent only. Data were normalized to expression levels of the *PPIA* housekeeping gene that did not change as a result of the PS administration. QPCR experiments were performed in triplicate. Error bars represent SEM ($n = 8$). Significant differences are indicated by $^{*}P < 0.05$, $^{**}P < 0.01$, $^{***}P < 0.005$ and $^{****}P < 0.0005$; Student's *t*-test.

IVS20+6T>C mutation (25). In order to analyse the splicing products of *IKBKAP* in the humanized knock-in FD mice, we isolated total RNA from dissected brain and liver tissues of the following genotypes: wt (*IKBKAP*$^{+/+}$), heterozygous humanized *IKBKAP* possessing the IVS20+6T>C (*IKBKAP*$^{FDloxP/+}$) and homozygous humanized *IKBKAP* with the IVS20+6T>C (*IKBKAP*$^{FDloxP/FDloxP}$). Quantitative real-time RT–PCR (QPCR) of the *IKBKAP* transcript in the *IKBKAP*$^{FDloxP/+}$ mice demonstrated a unique tissue-specific splicing pattern: *IKBKAP* is spliced differently in liver and brain in the three genotypes. In both tissues, the level of mRNA with exon 20 skipped is elevated in the homozygous mice compared with the wt mice; however, in the liver, the elevation was more significant (Fig. 1B). In both tissues, heterozygous mice displayed intermediate levels of inclusion and skipping of exon 20, suggesting that the FD*loxP*-modified humanized allele results in the reduction in the inclusion of exon 20 and elevation of the skipped isoform. In the brain of homozygous mice, the level of the mutant transcript was increased by 1.8-fold comparing with that in the wt mice, whereas in the liver of homozygous mice, the level of the skipped isoform was elevated by 2.5-fold. This indicates that the IVS20+6T>C mutation leads to tissue-specific exon skipping in the humanized FD mouse. However, in contrast to FD patients, in which the mutation leads to higher levels of exon skipping in the nervous system, in the FD mouse the mutation leads to higher levels of exon skipping in the liver than in the brain. A higher level of exon 20 skipping of the human *IKBKAP* gene in mouse liver compared with that of human was also shown in another humanized mouse model (25). This implies that there are differences in the mechanisms of regulation of exon 20 inclusion in the two species.

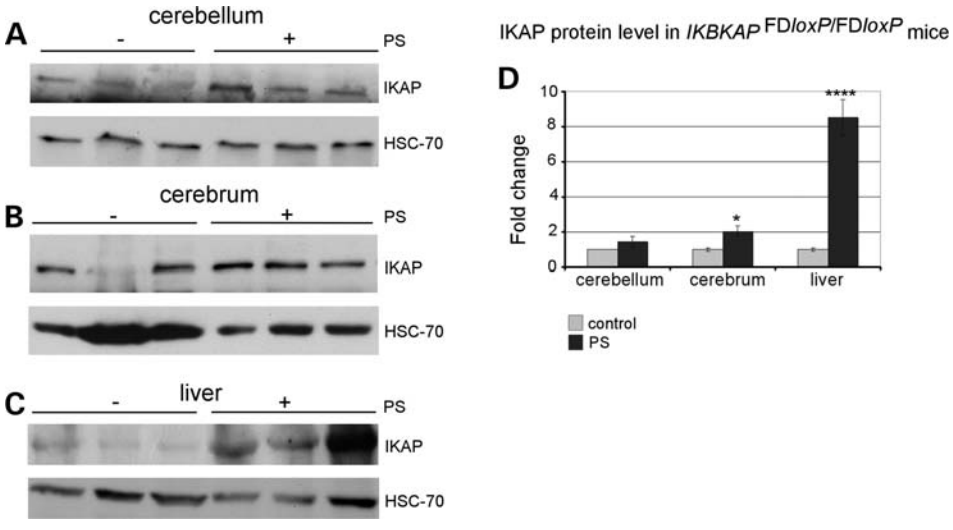

Figure 3. PS elevates IKAP protein levels in different tissues of *IKBKAP*$^{FDloxP/FDloxP}$ mice. (**A**–**C**) Western blotting of the cerebellum, cerebrum and liver lysates of *IKBKAP*$^{FDloxP/FDloxP}$ mice, using an anti-IKAP antibody (Anaspec) from mice treated with PS treatment (marked with a plus sign) and given solvent only (marked with a minus sign). The lower panels represent the same blots probed with HSC-70 antibody as a protein-loading control. (**D**) Bar charts show the fold change of IKAP expression based on the quantitation of western blots of cerebellum, cerebrum and liver tissues. White and black bars indicate control (vehicle only) and PS-treated mice, respectively. Error bars represent SEM ($n = 3$). Bands intensities were quantified using EZQuant-Gel v.2.2. Significant differences are indicated by $^{*}P < 0.05$ and $^{****}P < 0.0005$ (in the cerebellum $P = 0.068$).

The skipping level of exon 20 in the FD mouse is not sufficient to inflict disease symptoms; however, in the context of the mouse gene sequence, the IVS20+6T>C mutation leads to embryonic lethality (I. Dragatsis, personal communication). We aligned mouse and human exon 20 sequences and identified nine nucleotides that differ between the two species (Supplementary Material, Fig. S2A). Each of these positions in the mouse gene was mutated to the nucleotide observed in the human gene. Mutation of only one of the nine nucleotides restored a certain level of inclusion of exon 20 (Supplementary Material, Fig. S2A and B). This nucleotide is positioned in a putative binding site of the splicing factor SC35 (see Supplementary Material for further discussion). These results suggest that minor differences between human and mouse genomic sequences within the region of exon 19 through exon 21 result in differences in exon 20 selection. These data also imply that differences in functionality or expression level of splicing factors between the two species result in different levels of exon skipping. As exon 20 was alternatively spliced in a tissue-specific manner in the humanized FD mice, this model allowed us to test potential therapies for effects on the transcription level of *IKBKAP* and the extent of exon 20 inclusion.

PS elevates *IKBKAP* mRNA and IKAP protein levels in FD mice

FD is characterized by dysfunction of the autonomic and sensory nervous system resulting from incomplete neuronal development and progressive neuronal degeneration (32). We have searched for chemical candidates that affect neuronal function and would be safe for immediate testing in FD patients. One of the most promising substances we tested is PS (produced by Enzymotec under the Sharp·PS® brand). Cells derived from FD patients treated with PS had significantly higher levels of *IKBKAP* mRNA and IKAP protein than untreated cells (30). Therefore, we evaluated this substance in our *in vivo* model.

Eight FD mice were given 200 mg/kg Sharp·PS GOLD2008F (Enzymotec), a fluid PS-DHA compound, via gavage every other day, and eight FD mice were given solvent only, used as controls. Clinical studies demonstrated that extended treatment with PS improved efficiency (33). Hence, the mice were treated with PS for a period of 3 months. No visible phenotypic changes were observed in any of the PS-treated or control mice, and no significant changes in body weight occurred during the experiment. After 3 months, the mice were sacrificed, various tissues were harvested and total RNA was extracted and reverse-transcribed into cDNA. The splicing pattern of exon 20 was analysed by QPCR (Fig. 2).

The levels of the wt *IKBKAP* mRNA isoform in the cerebrum, cerebellum, heart and liver were significantly increased due to PS administration when compared with the vehicle-treated littermates. Figure 2 shows that the levels of the wt *IKBKAP* mRNA in the two neuronal tissues, cerebrum and cerebellum, were significantly increased by 1.4-fold when PS-treated animals were compared with untreated animals. In the heart and liver, PS administration resulted in increases of 2.5-fold. The levels of the mutant mRNA (exon 20 skipping isoform) were also elevated in the examined tissues (data not shown), suggesting that PS treatment affects transcription rather than splicing of *IKBKAP*. These findings are consistent with our previous results demonstrating that PS elevates the levels of both wt and mutant *IKBKAP* mRNA splicing isoforms in cells derived from FD patients (30). These results indicate that the non-neuronal tissues are more susceptible to the PS effect on mRNA levels than are neuronal tissues.

Next, we examined the impact of PS on IKAP protein levels by analysing extracts from the cerebrum, cerebellum, heart and liver by western blot (Fig. 3). The levels of IKAP protein in these tissues were remarkably increased in the

Table 1. GO analysis for up- and down-regulated genes in the cerebrum

GO term	Number of genes	FDR-corrected *P*-value
Cluster 1—Genes down-regulated following treatment with PS		
Mitochondrion—GO: 0005739	230	0.001
Ribosome—GO: 0005840	50	0.001
Mitochondrial part—GO: 0044429	80	0.001
Ribonucleoprotein complex—GO: 0030529	81	0.001
Translation—GO: 0006412	57	0.001
Ribosomal subunit—GO: 0033279	20	0.002
Large ribosomal subunit—GO: 0015934	15	0.002
Macromolecular complex—GO: 0032991	241	0.002
Intracellular organelle part—GO: 0044446	254	0.002
Cellular protein metabolic process—GO: 0044267	212	0.002
Organelle membrane—GO: 0031090	90	0.002
Cell redox homeostasis—GO: 0045454	18	0.003
Ribosome biogenesis—GO: 0042254	24	0.005
Neurotransmitter metabolic process—GO: 0042133	9	0.005
Amine metabolic process—GO: 0009308	47	0.007
Cytosolic part—GO: 0044445	16	0.009
Response to amphetamine—GO: 0001975	8	0.013
Establishment of localization—GO: 0051234	222	0.019
Macromolecule localization—GO: 0033036	100	0.02
Respiratory chain—GO: 0070469	16	0.03
Mitochondrial matrix—GO: 0005759	14	0.037
Cluster 2—genes up-regulated after treatment with PS		
Regulation of transcription—GO: 0045449	93	0.003
Regulation of metabolic process—GO: 0019222	116	0.003
Regulation of multicellular organismal process—GO: 0051239	45	0.003
Regulation of developmental process—GO: 0050793	43	0.006
Developmental process—GO: 0032502	112	0.006
Insulin-like growth factor binding—GO: 0005520	7	0.006
Negative regulation of biological process–GO: 0048519	62	0.007
Positive regulation of biological process—GO: 0048518	65	0.008
Regulation of transcription from RNA polymerase II promoter—GO: 0006357	37	0.017

Enriched categories were identified using DAVID to cluster differentially up- and down-regulated into functional categories using GO identification terms. Significant GO enrichment was obtained after FDR multiple testing correction ($P < 0.05$). See Supplementary Material, Table S1 for complete data.

PS-treated mice compared with the vehicle-treated littermates. In the cerebellum and cerebrum, PS supplementation increased the average level of IKAP protein by 1.45- and 2.05-fold, respectively. A dramatic increase was observed in the liver; IKAP protein levels were 8.51-fold higher in PS-treated mice than in controls. IKAP protein expression in all heart samples, including those of wt mice, was low, and we did not observe any substantial difference in expression levels between PS-treated and untreated mice (data not shown). It is important to note that PS treatment resulted in a heterogeneous effect on IKAP levels (Fig. 3). For instance, in the liver, the level of IKAP expression in PS-treated mice ranged from a change of 5.85-fold relative to the average of the untreated mice up to a change of 14.47-fold, whereas in the cerebrum and cerebellum, the values ranged from elevations of 1.2-fold up to 2-fold. Such heterogeneity was also observed in IKAP protein levels of mice treated with kinetin (34). We thus assume that PS treatment, like treatments with other therapeutic agents such as kinetin, affects mRNA levels differently in each individual.

Analysis of gene expression of cerebrum and heart tissues in PS-treated FD mice

To determine whether the expression of other genes was affected due to PS administration, we performed gene expression microarray analysis (Mouse Gene 1.0, Affymetrix) of cDNA samples from cerebrum and heart tissues of three FD mice. As controls, cDNA samples were taken from the same tissues of three FD mice supplemented with the solvent only. Using significance analysis of microarrays (SAM) (35), we identified 2401 genes with significantly different levels of expression in the cerebrum following PS treatment: 1746 genes were down-regulated after treatment with PS, and 655 were up-regulated. These genes are listed in Supplementary Material, Table S1A.

We clustered these genes based on changes in expression levels (Table 1). Within the cluster of genes that were down-regulated following treatment with PS, we observed a significant number of genes involved in two cellular functions: mitochondrial respiration and translation. We tested for functional enrichment by employing a hypergeomatric enrichment test for pathways from the Kyoto Encyclopedia of Genes and Genomes (KEGG) database (36). This analysis revealed a significant enrichment for genes involved in oxidative-phosphorylation, ribosomal and metabolic pathways (Fig. 4). There was also enrichment in genes known to be associated with Parkinson's disease; all of these genes were down-regulated after treatment with PS. These data suggest that PS should be considered as a treatment for other neurodegenerative diseases. We assume that the effect of PS treatment on gene expression of FD mouse will be similar to effects on wt animals such as the C57BL/6J strain, but this remains to be tested. The effect of PS on gene expression is probably not due to a specific effect on the *IKBKAP* gene splicing.

Our microarray analysis of gene expression in hearts of PS-treated and control FD mice demonstrated that only 100 genes were affected. Levels of 55 genes were up-regulated upon treatment with PS, and 45 genes were down-regulated. Functional analysis using TANGO revealed that five of the down-regulated genes are associated with chromatin organization (corrected P-value < 0.08). These genes are listed in Supplementary Material, Table S1B.

DISCUSSION

Here, we generated a humanized *IKBKAP* knock-in mouse with exon 20 and its two flanking introns with the major FD

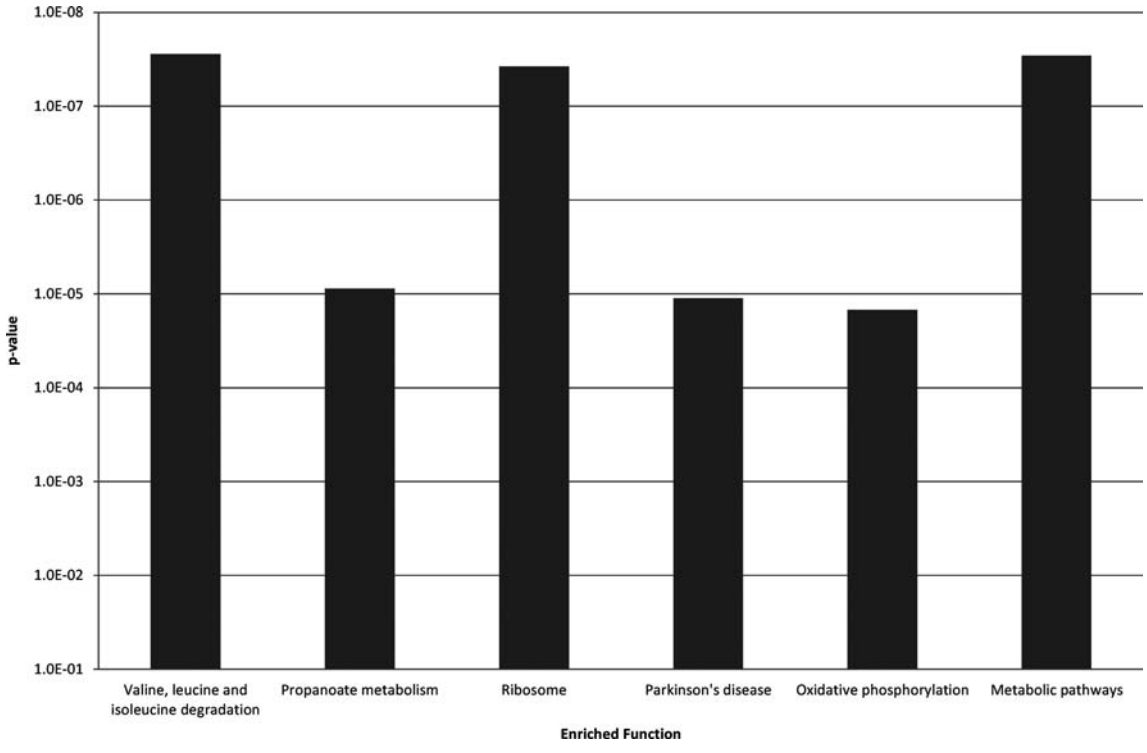

Figure 4. Significantly enriched signalling pathways in down-regulated genes in the cerebrum following PS treatment. The KEGG pathways database in DAVID was used to cluster up- and down-regulated genes. Significant KEGG enrichment ($P < 0.05$ after FDR multiple testing correction) was observed only for the down-regulated genes.

haplotype replacing the reciprocal sequence in the mouse *IKBKAP* gene. These mice were fully viable. Mice with the IVS20+6T>C mutation exhibited high levels of the skipped isoform of exon 20 in both the brain and liver. We treated these FD mice with PS, a lawful dietary supplement. Prolonged PS administration resulted in a substantial increase in both *IKBKAP* mRNA and protein levels in various tissues of the FD mice. PS derived from soy lecithin is currently given orally to human adults at a dosage of 200–300 mg per day and to children at 520 mg per day. The substance has been tested in humans and animals at a higher dose than recommended for use in humans with no toxicity observed (37–39). Therefore, we assume that administration of higher doses of PS to the FD mice would have led to a much more significant increase of both *IKBKAP* mRNA and protein levels without causing any toxicity effects.

The FD mice that we generated differ from other mouse models of FD (24–27). The IVS20+6T>C mutation introduced into the mouse genome resulted in embryonic lethality (I. Dragatsis, personal communication). We introduced a region of the human gene including exon 20 and its two flanking introns with the IVS20+6T>C mutation into mice. Our analysis of the human and mouse sequences and our studies of the effect of humanizing mutations showed that the IVS20+6T>C mutation impacts splicing and IKAP production differently in human and mouse, leading to a severe disease in human and to embryonic lethality in mouse. Our FD mouse demonstrates a different tissue-specific splicing pattern of *IKBKAP* gene compared with that observed in FD patients. In FD mice, we observed low exon 20 skipping levels in the brain and higher levels in the liver. Recent findings from Blencowe and co-workers revealed that splicing patterns of most genes located on human chromosome 21 are maintained in the reciprocal organs of mouse, indicating that cis-regulatory sequences control alternative splicing (40). However, certain splicing patterns were different between the mouse and human, implying that trans-splicing factors are involved in their regulation. Our results suggest that splicing of exon 20 in our FD mice is more susceptible to changes in *trans*-acting factors than to changes in *cis*-acting factors; we speculate that differences in concentrations of splicing factors between different organs of humans and mice result in the observed differences.

We used this humanized mouse to evaluate the effect of PS on the *IKBKAP* gene on three different levels: transcription, splicing and expression. Our results indicate that PS elevates the level of the *IKBKAP* mRNA in all tissues tested without affecting the ratio of exon 20 skipping and inclusion isoforms. This suggests that PS affects the level of transcription rather than splicing. The results also indicate that even a small increase in the level of *IKBKAP* mRNA is sufficient to elevate IKAP protein levels. The major impact of PS was detected in non-neuronal tissues. In neuronal tissues, *IKBKAP* mRNA levels increased significantly (1.4-fold increase), but to a lesser degree than in liver and heart (2.5-fold). Importantly, the amount of PS that crossed the blood–brain barrier (29) was sufficient to elevate both *IKBKAP* mRNA and IKAP protein levels. The PS effect was not the same on *IKBKAP* mRNA and IKAP protein: for example, in the cerebrum, PS treatment elevated *IKBKAP* mRNA level by 1.4-fold,

whereas the IKAP protein level was elevated by 2-fold. A more significant increase in protein than in mRNA levels was observed in the liver as well. We have previously demonstrated that cells from a parent of an FD patient (thus heterozygous for the IVS20+6T>C mutation) had a 60% reduction in *IKBKAP* mRNA compared with cells without such mutation—but no reduction in the IKAP protein level. Additionally, a 50% reduction in *IKBKAP* mRNA levels in the homozygous compared with heterozygous cells was observed, with non-detectable levels of the IKAP protein in the homozygous cells (30). A lack of correlation between mRNA and protein levels has been reported for other genes as well (41). It is important to note that PS might directly or indirectly affect *IKBKAP* mRNA export, nonsense-mediated decay activity, translational efficiency, or mRNA and/or protein stability. Indeed, effects at these other levels might also help to explain the lack of a tight correlation between mRNA and protein levels.

Apparently, there is a minimal threshold of the wt *IKBKAP* isoform necessary to generate a mouse with symptoms of FD disease. The levels of IKAP protein observed in tissues of the homozygous FD mice, in its neuronal tissues in particular, are apparently not low enough to result in symptoms characteristic of FD disease. Indeed, another mouse model for FD that was recently reported supports this notion as these mice, which have 5–10% of wt levels of IKAP, display some of FD symptoms (27). These mice developed FD features such as poor suckling and discoordination of swallow resulting in a significantly lower weight than their wt littermates. The transgenic mouse carrying the complete human *IKBKAP* locus with the FD IVS20+6T>C mutation does not exhibit detectable phenotypic features of FD (25). However, these mice did exhibit a tissue-specific splicing that replicates the pattern seen in FD patient tissues. Knock-out of the *IKBAKP* gene leads to embryonic lethality (24). Thus, there is a minimal threshold of IKAP that is critical for proper embryogenesis. On the other hand, when IKAP is synthesized above this threshold, mice grow up normally and do not display any FD-related phenotype.

Our gene expression array analysis revealed that levels of expression of an impressive number of genes were altered due to PS administration. This finding was not unexpected since a microarray analysis performed on cells derived from FD patients also revealed that PS resulted in an up-regulation of a variety of genes. A significant number of genes up-regulated by PS treatment were involved in cell-cycle regulation (30). However, the microarray analysis of the PS-treated FD mice did not confirm this result, probably due to the fact that developed neuronal cells, such as the ones analysed here, tend to remain in a permanent resting phase (G_0), and therefore are not expected to divide.

Our microarray expression analysis did show up-regulation of genes involved in transcription regulation after PS treatment. Interestingly, we also observed a significant down-regulation of genes encoding mitochondrial proteins. This finding may imply that there is a reduction in oxidative stress following treatment with PS. Although FD patients possess normal respiratory chain activity (42), oxidative stress may still be an important factor in FD (43). Down-regulation of ribosomal genes following treatment with PS may suggest that translation is more efficient post-treatment, which may also lead to a reduction in cell stress (44). This is further supported by the increase in transcription regulation-associated genes in the cerebrum of PS-treated mice (Table 1, Cluster 2). Strikingly, nearly 20% of genes up-regulated following treatment with PS are associated with at least one developmental process. This remarkable change in development-associated genes could signify an intrinsic change in cellular mechanisms, evident long after cells have matured, suggesting that supplementation of PS in early mouse embryonic stages may result in an improvement of neuronal development and survival. However, since our FD mouse model is fully viable, this assumption cannot be validated.

Our FD mouse is advantageous, since it has two *loxP* sequences that flank exon 20. This feature will allow us to create a conditional knock-out FD mouse, in which exon 20 will be deleted in a *Cre*-dependent manner (45). FD patients suffer from abnormal development and survival of the sensory and autonomic nervous system with progressive depletion of unmyelinated sensory and autonomic neurons (2,4,32). Thus, it is of interest to further elucidate the role of *IKBKAP* gene in the development of the peripheral nerve system by mating the FD mouse with a *Trp2-Cre* transgenic mouse (46), in which *Cre* is expressed exclusively in the peripheral nervous system.

The elevations in *IKBKAP* mRNA levels in the cerebrum, cerebellum, heart and liver of the FD mice treated with PS suggest that despite the lack of any physiological or clinical phenotypes, the generated FD mouse has an immense potential as a platform to evaluate therapeutic agents. It is important to note that despite the significant effect of PS on gene expression, such treatment was safe; none of the treated mice showed adverse symptoms. Our assumption is that by increasing the amount of the full-length IKAP protein among FD patients, their clinical status may be improved.

MATERIALS AND METHODS

Cloning of the mouse *IKBKAP* minigene

Primers were used to amplify the sequence from exon 19 through 21 of the *IKBKAP* gene. Both primers (Supplementary Material, Table S2; #3 and #4) contained an additional extension encoding a restriction enzyme sequence. The PCR product (853 bp) was digested with *Xho*I/*Pst*I and ligated into an *Xho*I/*Pst*I-cleaved pEGFP-C3 vector (Clontech) that contains the coding sequence for green fluorescent protein. Ligation was performed by using T4 DNA ligase (NEB). Colonies were screened with primers (#1 and #2) and verified by sequencing.

Site-directed mutagenesis

Nine positions in exon 20 of mouse *IKBKAP* minigene were substituted with corresponding human nucleotides by using PfuUltra II Fusion HS DNA Polymerase (Stratagene) as described in Carmel *et al.* (11). (Supplementary Material, Table S2; primers #10–27). The primer pair nomenclature indicates the position of the substituted nucleotide as shown

in Supplementary Material, Fig. S2A. The IVS20+6T>C mutation was induced in the mouse *IKBAKP* minigene using primers #5 and #6.

Cell culture, transfection and RT–PCR

The 293T and 3T3 cell lines were cultured in Dulbecco's modified Eagle's medium, supplemented with 4.5 g/ml glucose, 2 mM L-glutamine, 100 U/ml penicillin, 0.1 mg/ml streptomycin and 10% fetal calf serum (Biological Industries).

Cells were grown to 50% confluence in a 10 cm culture dish, under standard conditions, at 37°C with 5% CO_2. Cells were split at a 1:6 ratio into six-well plates 24 h prior to transfection. Transfection was performed using 3 μl of TransIT®-LT1 Transfection Reagent (Mirus) with 1 μg of plasmid DNA. Cells were harvested 48 h after transfection. Total cytoplasmic RNA was extracted using TriReagent (Sigma), followed by treatment with 2 U of DNase RNase-Free (Ambion). Reverse transcription was performed on 2 μg of total cytoplasmic RNA for 1 h at 42°C, using an oligo$(dT)_{20}$ and 2 U of avian myeloblastosis virus reverse transcriptase (Roche), according to the manufacturer's protocol. The spliced products derived from the expressed minigenes were detected by RT–PCR using primers located on the pEGFPC-3 plasmid (Supplementary Material, Table S2, primers #1 and #2). Amplification was performed for 30 cycles, consisting of 94°C for 30 s, 58°C for 45 s and 72°C for 1 min, using ready-mix (LAROVA). The products were resolved on a 1.5% agarose gel. Splicing products were eluted from gel and confirmed by sequencing after purification (Promega Wizard SV® gel PCR clean-up system).

Generation of the humanized knock-in *IKBKAP* $^{FDloxP/+}$ mouse

To obtain the full-length mouse genomic sequence of *IKBKAP*, we used the BAC clone, bMQ-389C23, carrying the genomic locus of *IKBKAP* (Geneservice), derived from AB2.2 embryonic stem cell DNA (129S7/SvEv Brd-Hprt b-m2) library. For the insertion of the corresponding human sequence, we used the human *IKBKAP* minigene containing the IVS20+6T>C mutation (11). We inserted a *loxP* site 20 nt downstream the 5′ss of exon 19 using PfuUltra II Fusion HS DNA Polymerase (Stratagene) (Supplementary Material, Table S2, primers #28 and #29).

We employed the recombineering approach in order to construct the conditional targeting vector (47,48). In brief, mouse exon 20 and its two flanking introns were deleted by *galK* cassette insertion (49). Then, we substituted the *galK* cassette with the human sequence of exon 20 and its two flanking introns, and 'retrieved' the human sequence along with ~10 kb genomic fragment from the mouse BAC into a PL253 vector (50,51). Lastly, the *Neo* cassette flanked by two FRT sites and a single *loxP* site was 'retrieved' by using an intermediate FRT vector to a PL253 vector as described in detail previously (52,53). After verification by sequencing, the final targeting vector was electroporated into 129/Sv mouse embryonic stem cells at the Transgenic and Gene Targeted Mice Unit of Weizmann Institute. Clones with successful recombination were identified by Southern blot analysis and were aggregated with an ICR donor morula. Blastocysts incorporated with positive embryonic stem cells were surgically implanted in the uteruses of pseudopregnant recipient mice. Chimeric males were bred to ICR females to determine germline transmission of the humanized allele. Offspring with an agouti/brownish-grey coat colour indicated a positive germline transmitter. The neomycin cassette was removed from intron 20 by crossing the humanized knock-in mice to a 129S4/SvJaeSor-*Gt(ROSA)26Sortm1(FLP1)Dym*/J (003946) Jackson line. The *IKBKAP*$^{FDloxP/+}$ was backcrossed to C57Bl/6J for five generations. A flowchart that describes the targeting of mouse *IKBKAP* gene is presented in Supplementary Material, Fig. S3.

The mice used in this study were housed in the animal facility of Tel Aviv University, provided with constant access to a standard diet of food and water, and maintained on a 12 h light/dark cycle. All experimental protocols were approved by the Animal Care and Use Committee of Tel Aviv University (number M-08-052).

Genotyping

Mice genotypes were determined by PCR analysis of genomic DNA from tail slips, using High Pure PCR Template Preparation Kit (Roche) according to the manufacturer's instructions. For distinguishing wt, heterozygous and homozygous mice, we used primers #7–9 (Supplementary Material, Table S2). Wt and homozygous *IKBKAP*$^{FDloxP/FDloxP}$ mice display genomic fragments of 1140 and 1392 bp, respectively, whereas heterozygous *IKBKAP* $^{FDloxP/+}$ mice display both fragments.

QPCR of *IKBKAP* transcripts

Mouse tissues (30 mg per sample) were frozen in liquid nitrogen and then homogenized with a Bio-Gen PR0-200® homogenizer. Purification of total RNA was performed using the RNeasy® Plus Mini Kit (QIAGEN), according to the manufacturer's protocol. RNA concentrations were determined using a NanoDrop ND-1000 spectrophotometer. Reverse transcription was performed on 0.5 μg of total RNA for 1 h at 50°C, using an oligo$(dT)_{20}$ primer and 200 U of SuperScript™ III RT (Invitrogen), according to the manufacturer's instructions.

Amplification was performed for 40 cycles, consisting two steps of 95°C for 30 s and 60°C for 3 s by using the Stratagene Mx3005P System and the KAPA SYBR® FAST QPCR master mix. Each reaction contained 50% QPCR mix and 0.2 μM primers in a total volume of 20 μl. Primers used to detect the *IKBKAP* wt isoform (inclusion of exon 20) and mutant isoform (skipping of exon 20) were #30–31 and #32–33, respectively. For normalization, we used the housekeeping gene *PPIA* (primers #34 and #35). Analysis was performed using the MxPro 4.01 software. All primer pairs yielded a linear standard curve with an $R^2 > 0.985$ and efficiency of reaction between 90 and 105%. All QPCR experiments were performed in triplicate.

Western blot analysis

Mouse tissues were homogenized on ice in RIPA buffer (50 mM Tris–HCl, pH 7.5, 1% NP40, 150 mM NaCl, 0.1%

SDS, 0.5% deoxycholic acid, 1 mM EDTA) containing protease inhibitor (Roche) and phosphatase inhibitor cocktails I and II (Sigma), using Bio-Gen PR0-200® homogenizer. Homogenates were left undisturbed on ice for 15 min. Supernatants containing proteins were collected after centrifugation for 30 min at 20 800*g* at 4°C, and protein concentrations were measured using the Bio-Rad Protein Assay (Bio-Rad). Total protein from the mouse liver, cerebrum (80 μg) and cerebellum (170 μg) were separated in an 8% SDS–PAGE and then electroblotted onto a Protran nitrocellulose transfer membrane (Schleicher & Schuell).

The membranes were blocked with 5% skim milk (Difco) in TBST for an hour at room temperature and probed with a rabbit anti-IKAP antibody (Anaspec, 1:500), rabbit anti-HSC70 (Abcam, 1:2000) for 12 h at 4°C, followed by washes and incubation with secondary antibody, donkey anti-rabbit (Abcam) HRP-conjugated (Jackson). Immunoblots were visualized by enhanced chemiluminescence (SuperSignal®, West Pico chemiluminescent substrate; Thermo Scientific, Pierce) and exposure to X-ray film (Super RX; Fuji).

PS administration by oral gavage

At 4 months of age, eight homozygous *IKBKAP*$^{FD loxP/FD loxP}$ mice were administrated with PS via oral gavage (each treatment included 200 mg/kg) every other day for a period of 3 months. In parallel, eight other *IKBKAP*$^{FD loxP/FD loxP}$ mice were supplemented only with the organic solvent medium-chain triglycerides (MCT); these mice were used as controls. PS (soy lecithin-derived, produced under the name Sharp·PS GOLD2008F) and the solvent were obtained from Enzymotec (http://www.sharp-ps.com/products/ps/ps.html) as liquids. Each oral dosing was performed with 100 μl of 200 mg/kg PS or 100 μl of MCT, using a 20 gauge bulb-tipped feeding needle (Fine Science Tools, Inc.). The mice were given food and water *ad libitum*, and changes in body weights were monitored on a daily basis.

Microarray analysis

Six Mouse Gene 1.0 microarray chips (Affymetrix) were used for the analysis of cDNA prepared from the cerebrum and heart of three individual *IKBKAP*$^{FD loxP/FD loxP}$ mice supplemented with PS, and six chips were used for the analysis of cDNA prepared from the cerebrum and heart of three individual *IKBKAP*$^{FD loxP/FD loxP}$ mice given solvent only. RNA was extracted from cerebrum and heart tissues using Qiagen RNeasy Plus Mini Kit, according to the manufacturer's protocol. cDNA and microarray chips were prepared and hybridized by the Bioinformatics Unit of Tel Aviv University. All microarray analyses were performed using the EXPANDER analysis platform (54). Raw microarray data were normalized using the robust multi-array average method (55), and mean expression was calculated for genes with more than one probe. Significantly differentially expressed genes were determined using the SAM technique (35) corrected for multiple testing using a false discovery rate of 0.05 (56). Genes were clustered into groups in an unsupervised manner using the CLICK algorithm (57) to yield two clusters with a total of 2401 genes (Supplementary Material, Table S1). To provide a comprehensive view of the effects of PS on live tissue, we also performed pathway analysis and functional analysis as described previously (54).

Statistical analysis

Comparisons between the PS treatment and control groups were performed using Student's *t*-test. Average means are represented as columns and the SEM is represented as error bars. The *P*-values and number of independent biological replicates (*n*) are indicated in the figure legends.

SUPPLEMENTARY MATERIAL

Supplementary Material is available at *HMG* online.

ACKNOWLEDGEMENTS

We are grateful to Dr Yonatan Manor and Dr Ariel Katz from Enzymotec for supplying the PS.

Conflict of Interest statement. None declared.

FUNDING

This work was supported by Dysautonomia Foundation, FD Hope, Israel FD Foundation, Israel Science Foundation (ISF Morasha 62/12; ISF 61/09; ISF Bikura 838/10). The funders had no rule in the study design, data collection and analysis, decision to publish or preparation of the manuscript.

REFERENCES

1. Lehavi, O., Aizenstein, O., Bercovich, D., Pavzner, D., Shomrat, R., Orr-Urtreqer, A. and Yaron, Y. (2003) Screening for familial dysautomia in Israel: evidence for higher carrier rate among Polish Ashkenazi Jews. *Genet. Test*, **7**, 139–142.
2. Slaugenhaupt, S.A. and Gusella, J.F. (2002) Familial dysautonomia. *Curr. Opin. Genet. Dev.*, **12**, 307–311.
3. Axelrod, F.B., Goldberg, J.D., Ye, X.Y. and Maayan, C. (2002) Survival in familial dysautonomia: impact of early intervention. *J. Pediatr.*, **141**, 518–523.
4. Axelrod, F.B. (2006) A world without pain or tears. *Clin. Auton. Res.*, **16**, 90–97.
5. Norcliffe-Kaufmann, L., Axelrod, F.B. and Kaufmann, H. (2011) Developmental abnormalities, blood pressure variability and renal disease in Riley Day syndrome. *J. Hum. Hypertens*, **27**, 51–55.
6. Norcliffe-Kaufmann, L., Axelrod, F. and Kaufmann, H. (2010) Afferent baroreflex failure in familial dysautonomia. *Neurology*, **75**, 1904–1911.
7. Macefield, V.G., Norcliffe-Kaufmann, L., Gutierrez, J., Axelrod, F.B. and Kaufmann, H. (2011) Can loss of muscle spindle afferents explain the ataxic gait in Riley-Day syndrome? *Brain*, **134**, 3198–3208.
8. Mendoza-Santiesteban, C.E., Hedges, T.R. III, Norcliffe-Kaufmann, L., Warren, F., Reddy, S., Axelrod, F.B. and Kaufmann, H. (2012) Clinical neuro-ophthalmic findings in familial dysautonomia. *J. Neuroophthalmol.*, **32**, 23–26.
9. Anderson, S.L., Coli, R., Daly, I.W., Kichula, E.A., Rork, M.J., Volpy, S.A., Ekstein, J. and Rubin, B.Y. (2001) Familial dysautonomia is caused by mutations of the IKAP gene. *Am. J. Hum. Genet.*, **68**, 753–758.
10. Rubin, B.Y. and Anderson, S.L. (2008) The molecular basis of familial dysautonomia: overview, new discoveries and implications for directed therapies. *Neuromol. Med.*, **10**, 148–156.
11. Carmel, I., Tal, S., Vig, I. and Ast, G. (2004) Comparartive analysis detects dependencies among the 5′ splice-site positoins. *RNA*, **10**, 828–840.

12. Cuajunco, M.P., Leyne, M., Mull, J., Gill, S.P., Gusella, J.F. and Slaugenhaupt, S.A. (2001) Cloning, characterization, and genomic structure of the mouse ikbkap gene. *DNA Cell Biol.*, **20**, 579–586.
13. Slaugenhaupt, S.A., Blumenfeld, A., Gill, S.P., Leyne, M., Mull, J., Cuajungco, M.P., Liebert, C.B., Chadwick, B., Idelson, M., Reznik, L. *et al.* (2001) Tissue-specific expression of a splicing mutation in the IKBKAP gene causes familial dysautonomia. *Am. J. Hum. Genet.*, **68**, 598–605.
14. Hawkes, N.A., Otero, G., Winkler, G.S., Marshall, N., Dahmus, M.E., Krappmann, D., Scheidereit, C., Thomas, C.L., Schiavo, G., Erdjument-Bromage, H. *et al.* (2002) Purification and characterization of the human elongator complex. *J. Biol. Chem.*, **277**, 3047–3052.
15. Holmberg, C., Katz, S., Lerdrup, M., Herdegen, T., Jaattela, M., Aronheim, A. and Kallunki, T. (2002) A novel specific role for I kappa B kinase complex-associated protein in cytosolic stress signaling. *J. Biol. Chem.*, **277**, 31918–31928.
16. Svejstrup, J.Q. (2007) Elongator complex: how many roles does it play? *Curr. Opin. Cell Biol.*, **19**, 331–336.
17. Nguyen, L., Humbert, S., Saudou, F. and Chariot, A. (2010) Elongator – an emerging role in neurological disorders. *Trends Mol. Med.*, **16**, 1–6.
18. Esberg, A., Huang, B., Johansson, M.J. and Bystrom, A.S. (2006) Elevated levels of two tRNA species bypass the requirement for elongator complex in transcription and exocytosis. *Mol. Cell*, **24**, 139–148.
19. Rahl, P.B., Chen, C.Z. and Collins, R.N. (2005) Elp1p, the yeast homolog of the FD disease syndrome protein, negatively regulates exocytosis independently of transcriptional elongation. *Mol. Cell*, **17**, 841–853.
20. Johansen, L.D., Naumanen, T., Knudsen, A., Westerlund, N., Gromova, I., Junttila, M., Nielsen, C., Bottzauw, T., Tolkovsky, A., Westermarck, J. *et al.* (2008) IKAP localizes to membrane ruffles with filamin A and regulates actin cytoskeleton organization and cell migration. *J. Cell Sci.*, **121**, 854–864.
21. Close, P., Hawkes, N., Cornez, I., Creppe, C., Lambert, C.A., Rogister, B., Siebenlist, U., Merville, M.P., Slaugenhaupt, S.A., Bours, V. *et al.* (2006) Transcription impairment and cell migration defects in elongator-depleted cells: implication for familial dysautonomia. *Mol. Cell*, **22**, 521–531.
22. Cheishvili, D., Maayan, C., Smith, Y., Ast, G. and Razin, A. (2007) IKAP/hELP1 deficiency in cerebrum of familial dysautonomia patients results in down regulation of genes involved in oligodendrocyte differentiation and in myelination. *Human Mol. Genet.*, **16**, 2097–2104.
23. Cornez, I., Creppe, C., Gillard, M., Hennuy, B., Chapelle, J.P., Dejardin, E., Merville, M.P., Close, P. and Chariot, A. (2008) Deregulated expression of pro-survival and pro-apoptotic p53-dependent genes upon Elongator deficiency in colon cancer cells. *Biochem. Pharmacol.*, **75**, 2122–2134.
24. Chen, Y.T., Hims, M.M., Shetty, R.S., Mull, J., Liu, L., Leyne, M. and Slaugenhaupt, S.A. (2009) Loss of mouse Ikbkap, a subunit of elongator, leads to transcriptional deficits and embryonic lethality that can be rescued by human IKBKAP. *Mol. Cell Biol.*, **29**, 736–744.
25. Hims, M.M., Shetty, R.S., Pickel, J., Mull, J., Leyne, M., Liu, L., Gusella, J.F. and Slaugenhaupt, S.A. (2007) A humanized IKBKAP transgenic mouse models a tissue-specific human splicing defect. *Genomics*, **90**, 389–396.
26. Dietrich, P., Yue, J., Shuyu, E. and Dragatsis, I. (2011) Deletion of exon 20 of the familial dysautonomia gene Ikbkap in mice causes developmental delay, cardiovascular defects, and early embryonic lethality. *PLoS One*, **6**, e27015.
27. Dietrich, P., Alli, S., Shanmugasundaram, R. and Dragatsis, I. (2012) IKAP expression levels modulate disease severity in a mouse model of familial dysautonomia. *Hum. Mol. Genet.*, **21**, 5078–5090.
28. Vance, J.E. and Steenbergen, R. (2005) Metabolism and functions of phosphatidylserine. *Prog. Lipid. Res.*, **44**, 207–234.
29. US Food and Drug Administration website: http://www.fda.gov/Food/LabelingNutrition/LabelClaims/QualifiedHealthClaims/ucm072999.htm. Accessed 10 February 2013.
30. Keren, H., Donyo, M., Zeevi, D., Maayan, C., Pupko, T. and Ast, G. (2010) Phosphatidylserine increases IKBKAP levels in familial dysautonomia cells. *PLoS One*, **5**, e15884.
31. Slaugenhaupt, S.A. (2002) Genetics of familial dysautonomia tissue-specific expression of a splicing mutation in the IKBKAP gene. *Clin. Auton. Res.*, **12**, 15–19.
32. Axelrod, F.B. (2004) Familial dysautonomia. *Muscle Nerve*, **29**, 352–363.
33. Pepeu, G., Pepeu, I.M. and Amaducci, L. (1996) A review of phosphatidylserine pharmacological and clinical effects. Is phosphatidylserine a drug for the ageing brain? *Pharmacol. Res.*, **33**, 73–80.
34. Shetty, R.S., Gallagher, C.S., Chen, Y.T., Hims, M.M., Mull, J., Leyne, M., Pickel, J., Kwok, D. and Slaugenhaupt, S.A. (2011) Specific correction of a splice defect in brain by nutritional supplementation. *Hum. Mol. Genet.*, **20**, 4093–4101.
35. Tusher, V.G., Tibshirani, R. and Chu, G. (2001) Significance analysis of microarrays applied to the ionizing radiation response. *Proc. Natl Acad. Sci. USA*, **98**, 5116–5121.
36. Kanehisa, M. and Goto, S. (2000) KEGG: Kyoto Encyclopedia of Genes and Genomes. *Nucleic. Acids Res.*, **28**, 27–30.
37. Jorissen, B.L., Brouns, F., Van Boxtel, M.P. and Riedel, W.J. (2002) Safety of soy-derived phosphatidylserine in elderly people. *Nutr. Neurosci.*, **5**, 337–343.
38. Kingsley, M. (2006) Effects of phosphatidylserine supplementation on exercising humans. *Sports Med.*, **36**, 657–669.
39. Ohkubo, T. and Tanaka, Y. (2010) Administration of DHA-PS to aged mice was suitable for increasing hippocampal PS and DHA ratio. *J. Oleo. Sci.*, **59**, 247–253.
40. Barbosa-Morais, N.L., Irimia, M., Pan, Q., Xiong, H.Y., Gueroussov, S., Lee, L.J., Slobodeniuc, V., Kutter, C., Watt, S., Colak, R. *et al.* (2012) The evolutionary landscape of alternative splicing in vertebrate species. *Science*, **338**, 1587–1593.
41. Gry, M., Rimini, R., Stromberg, S., Asplund, A., Ponten, F., Uhlen, M. and Nilsson, P. (2009) Correlations between RNA and protein expression profiles in 23 human cell lines. *BMC Genomics*, **10**, 365.
42. Strasberg, P., Bridge, P., Merante, F., Yeger, H. and Pereira, J. (1996) Normal mitochondrial DNA and respiratory chain activity in familial dysautonomia fibroblasts. *Biochem. Mol. Med.*, **59**, 20–27.
43. Gardiner, J., Barton, D., Overall, R. and Marc, J. (2009) Neurotrophic support and oxidative stress: converging effects in the normal and diseased nervous system. *Neuroscientist*, **15**, 47–61.
44. Vogel, C., Silva, G.M. and Marcotte, E.M. (2011) Protein expression regulation under oxidative stress. *Mol. Cell Proteomics*, **10**, M111 009217.
45. Lewandoski, M. (2001) Conditional control of gene expression on the mouse. *Nat. Rev. Genet.*, **2**, 743–755.
46. Zhao, S. and Overbeek, P.A. (1999) Tyrosinase-related protein 2 promoter targets transgene expression to ocular and neural crest-derived tissues. *Dev. Biol.*, **216**, 154–163.
47. Copeland, N.G., Jenkins, N.A. and Court, D.L. (2001) Recombineering: a powerful new tool for mouse functional genomics. *Nat. Rev. Genet.*, **2**, 769–779.
48. Court, D.L., Sawitzke, J.A. and Thomasson, L.C. (2002) Genetic engineering using homologous recombination. *Annu. Rev. Genet.*, **36**, 361–388.
49. http://ncifrederick.cancer.gov/research/brb/protocol/Protocol3_SW102_galK_v2.pdf. Accessed 10 February 2013.
50. Liu, P., Jenkins, N.A. and Copland, N.G. (2003) A highly efficient recombineering-based method for generating conditional knockout mutations. *Genome Res.*, **13**, 476–484.
51. http://web.ncifcrf.gov/research/brb/productDataSheets/recombineering/plasmid/PL253_map.pdf. Accessed 10 February 2013.
52. http://ncifrederick.cancer.gov/research/brb/protocol/Protocol4_CKO_design.pdf. Accessed 10 February 2013.
53. http://web.ncifcrf.gov/research/brb/productDataSheets/recombineering/plasmid/PL451_map.pdf. Accessed 10 February 2013.
54. Shamir, R., Maron-Katz, A., Tanay, A., Linhart, C., Steinfeld, I., Sharan, R., Shiloh, Y. and Elkon, R. (2005) EXPANDER—an integrative program suite for microarray data analysis. *BMC Bioinformatics*, **6**, 232.
55. Irizarry, R.A., Hobbs, B., Collin, F., Beazer-Barclay, Y.D., Antonellis, K.J., Scherf, U. and Speed, T.P. (2003) Exploration, normalization, and summaries of high density oligonucleotide array probe level data. *Biostatistics*, **4**, 249–264.
56. Benjamini, Y., Drai, D., Elmer, G., Kafkafi, N. and Golani, I. (2001) Controlling the false discovery rate in behavior genetics research. *Behav. Brain Res.*, **125**, 279–284.
57. Sharan, R. and Shamir, R. (2000) CLICK: a clustering algorithm with applications to gene expression analysis. *Proc. Int. Conf. Intell. Syst. Mol. Biol.*, **8**, 307–316.